Optimized max-dmin precoder assuming maximum squared Euclidean weight-mapping and turbo detection

Nhat Quang Nhan, Philippe Rostaing, Karine Amis Cavalec, Ludovic Collin, Emanuel Radoi

Optimized $\max$-$d_{\min}$ precoder assuming maximum squared Euclidean weight-mapping and turbo detection

Nhat-Quang Nhan*†, Philippe Rostaing*, Karine Amis†, Ludovic Collin*, and Emanuel Radoi*
* Université Européenne de Bretagne; Université de Brest; CNRS, UMR 6285 Lab-STICC, France,
Email: {nhat-quang.nhan, philippe.rostaing, ludovic.collin, emanuel.radoi}@univ-brest.fr
† Institut Mines-Telecom; Telecom Bretagne; Signal and Communications department;
CNRS, UMR 6285 Lab-STICC, Technopôle Brest-Iroise CS 83818, 29238 Brest Cedex 3, France,
Email: {nhat.nhan, karine.amis}@telecom-bretagne.eu

***Abstract*—The concatenation of multiple-input multiple-output (MIMO) linear precoder with an outer forward error correction (FEC) encoder is investigated at the transmitter. Turbo detection is applied at the receiver for the decoding. The bit-interleaved codeword is considered to be grouped and mapped directly onto the received constellation thanks to a MIMO symbol mapper. We exploit the optimal maximum squared Euclidean weight (MSEW) mappings for two forms of $\max$-$d_{\min}$ precoder to propose a novel precoder referred to as $\max$-$\ell_{\min}$. The switching threshold between both forms is optimized by considering all received sequences whose binary mappings differ by exactly one bit and by first maximizing the minimum Euclidean distance within this set and then minimizing the number of pairs achieving it. Extrinsic information transfer (EXIT) chart is also used to validate the analysis. Simulation results show significant improvement, in terms of system error-rate performance, of the $\max$-$\ell_{\min}$ compared to the conventional $\max$-$d_{\min}$.**

***Index Terms*—Linear MIMO precoder, turbo detection, iterative receiver.**

I. Introduction

Deploying multiple antennas at both transmitter and receiver of a wireless link (MIMO) is one of the key technology to tackle the challenges of higher data rate and increasing data traffic that the modern radio-cellular networks have to face up [1]. In time domain duplex (TDD) closed-loop schemes, the channel state information (CSI) is readily available at the transmitter through a feedback link, which enables to design a precoder that adapts to the channel conditions by exploiting the multiple antennas at the transmitter. Additionally, the turbo detection, which applies the well-known turbo principle [2], shows a great advantage to combat intersymbol interference. It was firstly introduced in [3] and later applied in many MIMO systems [4]. A turbo detection scheme contains a soft demapper block and a soft FEC decoder block, which exchange extrinsic information to improve the detection and decoding processes at each iteration and, finally, enhance error-rate performance at the convergence. In this paper, we consider the concatenation of the MIMO precoder with a binary recursive systematic convolutional code assuming turbo detection at the receiver. We assume perfect CSI at both the transmitter and the receiver.

We start from the two forms of the max-d_{min} precoder [5], respectively referred to as $\mathbf{F}_{r_1}$ or $\mathbf{F}_{octa}$ and we aim at optimizing the switching threshold from one to another. The $\max$-$d_{\min}$ precoder was initially designed to maximize the minimum Euclidean distance between two received sequences assuming a Gray-mapping and no outer FEC code. For both $\mathbf{F}_{r_1}$ and $\mathbf{F}_{octa}$, the received constellation is fixed and is only scaled by a positive factor depending on a channel parameter γ explained hereinafter in the paper, which enables a MIMO mapper design that maps directly the encoded binary sequence onto the received constellation [6]. In [6], we individually optimized the MSEW-mapping for both $\mathbf{F}_{r_1}$ and $\mathbf{F}_{octa}$. Taking into account the outer FEC and a turbo detection, we analyzed the ending point of the EXIT chart for lower error-floor purpose and observed that beyond a given value of the parameter γ, both precoders achieve the same ending point, making the switching threshold useless. The resulting MSEW-mapped $\max$-$d_{\min}$ precoder outperforms all Gray-mapped $\max$-$d_{\min}$ precoders [1]. In this paper, to further enhance the error-rate performance, we define a switching threshold between MSEW-mapped $\mathbf{F}_{r_1}$ and $\mathbf{F}_{octa}$ so as to maximize the minimum Euclidean distance between two received sequences whose binary mappings differ by exactly one bit. We refer to the new precoder as $\max$-$\ell_{\min}$ precoder. EXIT charts as well as error rate simulations carried over random MIMO channels support the analysis.

The remainder of this paper is organized as follows. Section II briefly introduces the system model along with $\max$-$d_{\min}$ MIMO precoder. In Section III, the optimal MSEW mappings at the received constellations of $\max$-$d_{\min}$ precoder are firstly recalled. Subsequently, the new $\max$-$\ell_{\min}$ precoder is proposed. Also in this section, EXIT chart analysis is introduced for verification. Simulated error rates are presented in Section IV to validate the analysis. Section V concludes the paper and gives some perspectives.

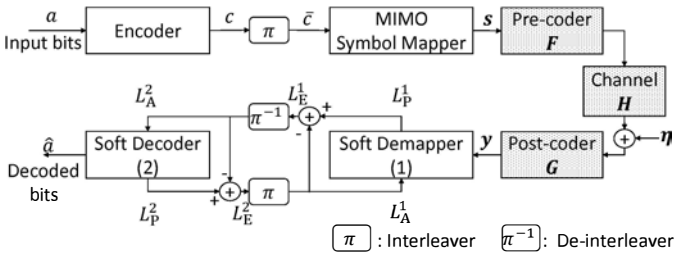

Fig. 1: System model.

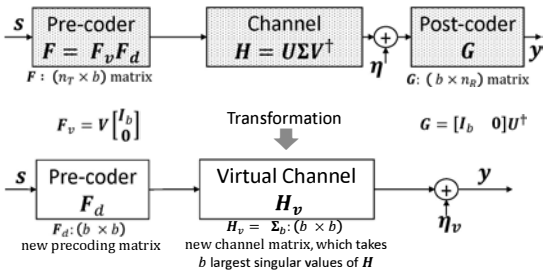

Fig. 2: Equivalent channel transformation.

II. System model and preliminaries

A. System model

Let us consider a MIMO system with n_R receive, n_T transmit antennas and b independent data streams to be transmitted. A binary recursive-systematic convolutional (RSC) code is used to encode the information binary sequence. The FEC codeword is interleaved before entering a MIMO symbol mapper. In the MIMO symbol mapper, interleaved FEC-encoded bits are grouped into packets and each packet is mapped onto a b-dimensional symbol vector $\mathbf{s}$. The vector $\mathbf{s}$ is then precoded with a precoding matrix $\mathbf{F}$ and transmitted through the MIMO channel. At the receiver side, after MIMO detection, a soft symbol demapper iteratively exchanges extrinsic information with a BCJR soft decoder [7]. The detection output, denoted by $\mathbf{y}$, reads

$$\mathbf{y} = \mathbf{GHFs} + \mathbf{G}\boldsymbol{\eta}, \tag{1}$$

where $\mathbf{F}$ is the $n_T \times b$ precoding matrix with the power constraint $\|\mathbf{F}\|_F^2 = 1$, $\|.\|_F$ is the Frobenius norm, $\mathbf{G}$ is the $b \times n_R$ postcoding matrix, $\mathbf{H}$ is the $n_R \times n_T$ channel matrix, and $\boldsymbol{\eta}$ is the $n_R \times 1$ additive white circularly-symmetric complex gaussian noise vector. Let $E[.]$ and $(.)^\dagger$ stand for the expectation and the conjugate transpose respectively and let $\mathbf{I}_{n_R}$ be the identity matrix of size n_R. Then we assume $E[\boldsymbol{\eta}\boldsymbol{\eta}^\dagger] = \sigma_\eta^2 \mathbf{I}_{n_R}$ and $E[\mathbf{ss}^\dagger] = \sigma_s^2 \mathbf{I}_b$. The system model is shown in Fig. 1, where L_A^1, L_P^1 and L_E^1 respectively stand for the *a priori*, the *a posteriori* and the extrinsic log likelihood ratios (LLRs) of the soft demapper, while the equivalent notations for the BCJR soft decoder are L_A^2, L_P^2 and L_E^2.

According to [5], the following channel transformation is applied to simplify the system model. Let us define $\mathbf{F}_d$ and $\mathbf{F}_v$ such that $\mathbf{F} = \mathbf{F}_v \times \mathbf{F}_d$. Matrices $\mathbf{F}_v$ and $\mathbf{G}$ are unitary and chosen so as to transform the MIMO channel into a virtual channel with b independent parallel sub-channels, *i.e.* the columns of $\mathbf{F}_v$ and $\mathbf{G}^\dagger$ respectively are the b most significant right-singular and left-singular vectors of the singular value decomposition of $\mathbf{H}$. Note that $\mathbf{F}_d$ denotes the new precoding matrix. It also satisfies the power constraint $\|\mathbf{F}_d\|_F^2 = 1$. The equivalent model is written as

$$\mathbf{y} = \mathbf{H}_v \mathbf{F}_d \mathbf{s} + \boldsymbol{\eta}_v, \tag{2}$$

where $\boldsymbol{\eta}_v$ is the $b \times 1$ virtual noise vector with $\mathrm{E}[\boldsymbol{\eta}_v \boldsymbol{\eta}_v^\dagger] = \sigma_\eta^2 \mathbf{I}_b$. The matrix $\mathbf{H}_v = \mathrm{diag}(\sigma_1, ..., \sigma_b)$ is the $b \times b$ eigen-channel matrix, where $\{\sigma_1, ..., \sigma_b\}$ are the b most significant singular values of $\mathbf{H}$ sorted in descending order. The received constellation symbol is now defined by $\mathbf{x} = \mathbf{H}_v \mathbf{F}_d \mathbf{s}$. A demonstration for the channel transformation is shown in Fig. 2. The transformation above only requires $b \leq \mathrm{rank}(\mathbf{H}) \leq \min(n_T, n_R)$, therefore, it is important to note that n_T and n_R can be larger than b. In this paper, we restrict ourselves to $b = 2$. The conversion from cartesian to polar form of $\mathbf{H}_v$ gives

$$\mathbf{H}_v = \begin{pmatrix} \sigma_1 & 0 \\ 0 & \sigma_2 \end{pmatrix} = \rho \begin{pmatrix} \cos\gamma & 0 \\ 0 & \sin\gamma \end{pmatrix}, \tag{3}$$

where ρ and γ respectively represent the channel gain and angle. As $\sigma_1 \geq \sigma_2 > 0$, we have $0 < \gamma \leq \pi/4$. Therefore, any random MIMO channel can be simply characterized by the pair (ρ, γ) thanks to the virtual transformation. Let us define the instantaneous received SNR as

$$\mathrm{SNR} = \frac{\sigma_s^2}{\sigma_\eta^2} \|\mathbf{H}\|_F^2 = \frac{\sigma_s^2}{\sigma_\eta^2} \rho^2. \tag{4}$$

With this definition of SNR, a channel is only characterized by its angle γ.

In most MIMO coded schemes, a binary to M-ary symbol conversion is inserted between the FEC code and the MIMO precoder. Traditionally, the interleaved FEC codeword is mapped onto mono-dimensional M-ary modulated symbols. The mapped symbols are then converted into a b-dimensional symbol vector $\mathbf{s}$. In contrast to the conventional mapping, in this paper, we apply the work in [6] by considering a direct mapping of the interleaved FEC codeword into $\mathbf{s}$. Note that elements of $\mathbf{s}$ are M-ary modulated symbols. We denote by $\mathcal{Q}$ the set of all symbol vectors $\mathbf{s}$. Then, the size of $\mathcal{Q}$ is M^b. The process at soft demapper of the well-known MIMO turbo detection scheme, which is widely applied in many research papers [4], is not presented here due to space limitation.

B. The $\max\text{-}d_{\min}$ linear precoder

We focus on a commonly used precoder named $\max\text{-}d_{\min}$ [5], in which, $\mathbf{F}_d$ was designed to maximize the minimum Euclidean distance, which is denoted by $d_{\min} = \min_{m \neq \ell} \|\mathbf{x}_m - \mathbf{x}_\ell\|$ where $\mathbf{x} = \mathbf{H}_v \mathbf{F}_d \mathbf{s}$, between the received constellation symbols. In case $b = 2$ and 4-QAM modulation, the optimal solution depends on γ and by defining the threshold $\gamma_0 = \arctan\sqrt{\frac{\sqrt{2}-1}{2\sqrt{2}+\sqrt{6}-1}}$ ($\approx 17,28^0$), $\mathbf{F}_d$ reads

- if $0 \leq \gamma \leq \gamma_0$

$$\mathbf{F}_d = \mathbf{F}_{r_1} = \begin{pmatrix} \sqrt{\frac{3+\sqrt{3}}{6}} & \sqrt{\frac{3-\sqrt{3}}{6}} e^{i\frac{\pi}{12}} \\ 0 & 0 \end{pmatrix}, \tag{5}$$

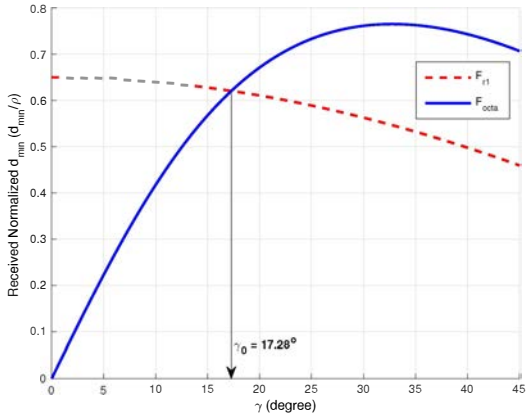

Fig. 3: The received normalized $d_{\min}$ versus γ.

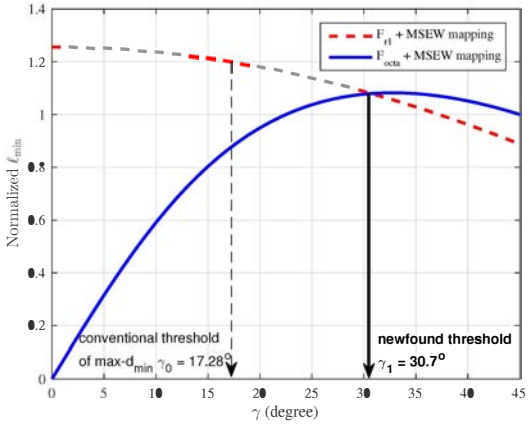

Fig. 4: Normalized $\ell_{\min}$ versus γ with MSEW mappings.

- if $\gamma_0 < \gamma \leq \pi/4$

$$\mathbf{F}_d = \mathbf{F}_{octa} = \tfrac{1}{\sqrt{2}} \begin{pmatrix} \cos\psi & 0 \\ 0 & \sin\psi \end{pmatrix} \begin{pmatrix} 1 & e^{i\frac{\pi}{4}} \\ -1 & e^{i\frac{\pi}{4}} \end{pmatrix}, \quad (6)$$

where $\psi = \arctan \frac{\sqrt{2}-1}{\tan\gamma}$. Apparently, in the case $\gamma \leq \gamma_0$, *i.e.* $\mathbf{F}_d = \mathbf{F}_{r_1}$, the precoder only spreads power on the first sub-channel. In the case $\gamma > \gamma_0$, *i.e.* $\mathbf{F}_d = \mathbf{F}_{octa}$, the precoder spreads power on both sub-channels.

Fig 3 shows the received $d_{\min}$ normalized by ρ of $\mathbf{F}_{r1}$ and $\mathbf{F}_{octa}$. We can see that, in order to keep the high value of the received normalized $d_{\min}$, the max-$d_{\min}$ precoder uses γ_0 as a threshold to switch between $\mathbf{F}_{r1}$ and $\mathbf{F}_{octa}$. Note that γ_0 is SNR-independent and designed for uncoded system. The study of this threshold for the turbo detection, under assumption of optimized mapping at the MIMO symbol mapper, will be presented in Section III-B.

III. Analysis

A. Influence of mapping at the received constellation

From (3) and the precoding matrix (5) or (6), it comes that $\mathbf{H}_v\mathbf{F}_d = a\mathbf{A}$, where $\mathbf{A}$ is a fixed matrix and a is a scalar, which depends on γ and ρ. Therefore, the received constellation (of $\mathbf{F}_{r1}$ or $\mathbf{F}_{octa}$) is unchanged and just scaled by a scalar factor a for each channel. Consequently, at the MIMO symbol mapper, grouping and mapping the encoded binary bits into $\mathbf{s}$ is equivalent to map the encoded bits onto the received constellation symbol, which is defined by $\mathbf{x} = \mathbf{H}_v\mathbf{F}_d\mathbf{s}$.

The selected mapping depends on a key parameter denoted by ℓ and defined as

$$\ell(\breve{\mathbf{s}}, \breve{\mathbf{s}}') = \|\mathbf{H}_v\mathbf{F}_d(\breve{\mathbf{s}} - \breve{\mathbf{s}}')\|^2, \quad (7)$$

where $\breve{\mathbf{s}}$ and $\breve{\mathbf{s}}'$ represent any pair of symbol vectors with associated binary conversions differing by exactly one bit. The minimum value of ℓ over the received constellation is denoted by $\ell_{\min}$. At high SNR, we deduce that the fault detections, which may lead to errors in the iterative process of the turbo detection, mostly occur between the pair of received constellation symbols separated by $\ell_{\min}$. Indeed, it is shown in [6] that maximizing $\ell_{\min}$ results in a significant error-rate

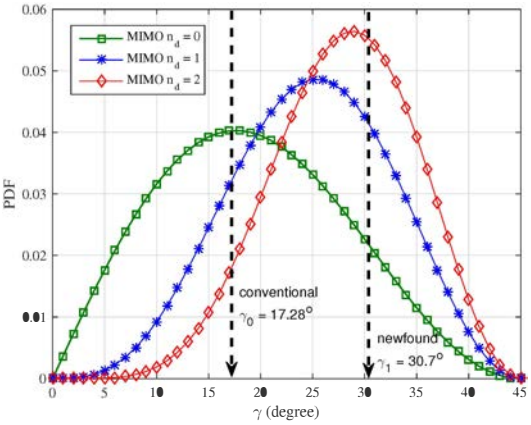

Fig. 5: Probability density functions in terms of γ of different MIMO configurations with $b = 2$ data streams, where $n_d = |n_T - n_R|$ and $\min\{n_T, n_R\} = 2$.

performance improvement for the max-$d_{\min}$ precoded MIMO system assuming turbo detection at the receiver. The MSEW mapping proposed in [8] consists in first maximizing $\ell_{\min}$ and then minimizing the number of pairs $(\breve{\mathbf{s}}, \breve{\mathbf{s}}')$ such that $\ell(\breve{\mathbf{s}}, \breve{\mathbf{s}}') = \ell_{\min}$.

Let us recall the optimal MSEW mappings for $\mathbf{F}_{r1}$ and $\mathbf{F}_{octa}$ that we obtained in [6]. By denoting 16 possible values of $\mathbf{s}$ by $\mathbf{s}_0 = [s_0\ s_0]^{\mathrm{T}}$, $\mathbf{s}_1 = [s_0\ s_1]^{\mathrm{T}}$, $\mathbf{s}_2 = [s_0\ s_2]^{\mathrm{T}}$, $\mathbf{s}_3 = [s_0\ s_3]^{\mathrm{T}}$, $\mathbf{s}_4 = [s_1\ s_0]^{\mathrm{T}}$, $\mathbf{s}_5 = [s_1\ s_1]^{\mathrm{T}}$, $\mathbf{s}_6 = [s_1\ s_2]^{\mathrm{T}}$, $\mathbf{s}_7 = [s_1\ s_3]^{\mathrm{T}}$, $\mathbf{s}_8 = [s_2\ s_0]^{\mathrm{T}}$, $\mathbf{s}_9 = [s_2\ s_1]^{\mathrm{T}}$, $\mathbf{s}_{10} = [s_2\ s_2]^{\mathrm{T}}$, $\mathbf{s}_{11} = [s_2\ s_3]^{\mathrm{T}}$, $\mathbf{s}_{12} = [s_3\ s_0]^{\mathrm{T}}$, $\mathbf{s}_{13} = [s_3\ s_1]^{\mathrm{T}}$, $\mathbf{s}_{14} = [s_3\ s_2]^{\mathrm{T}}$ and $\mathbf{s}_{15} = [s_3\ s_3]^{\mathrm{T}}$, where $s_0 = (-1-i)/\sqrt{2}$, $s_1 = (-1+i)/\sqrt{2}$, $s_2 = (1-i)/\sqrt{2}$, $s_3 = (1+i)/\sqrt{2}$ and $[.]^{\mathrm{T}}$ stands for vector transposition, the bit-interleaved encoded bits of $\bar{c}$ are grouped into length-4 packets and mapped directly onto $\mathbf{s}$. Then, the optimal mappings for $\mathbf{F}_{r1}$ and $\mathbf{F}_{octa}$ are presented in TABLE I. Note that, in this table, the Gray-direct mapping stands for the conventional mapping that Gray-maps every 2 encoded bits into one 4-QAM symbol before converting the modulated symbols to the b-dimensional symbol vector $\mathbf{s}$ ($b = 2$) using parallel to symbol converter.

TABLE I: The optimized binary representation in the constellation map of precoder max-$d_{\min}$ for different mappings (each decimal value represents for 4 binary bits, *e.g.* $(8)_{10} = (1000)_2$) [6].

Mapping	Mode	$\mathbf{s}_0 \dots \mathbf{s}_i \dots \mathbf{s}_{15}$
Gray-direct	$\mathbf{F}_{r_1/octa}$	[0 1 2 3 4 5 6 7 8 9 10 11 12 13 14 15]
MSEW	$\mathbf{F}_{r_1}$	[7 2 1 11 13 4 8 14 12 6 10 15 5 3 0 9]
	$\mathbf{F}_{octa}$	[2 5 7 0 9 12 10 15 11 14 8 13 4 3 1 6]

B. Optimized max-$\ell_{\min}$ *precoder*

In this subsection, we propose an optimization for max-$d_{\min}$ precoder in turbo detection scheme. The precoder optimization relies on the received constellations. We first remind that considering $\mathbf{F}_{r_1}$ or $\mathbf{F}_{octa}$, the received constellation is fixed and scaled by a positive factor a which depends always on γ.

Assuming no outer FEC code and a Gray-mapping, the max-$d_{\min}$ precoder defined in [5] switches between $\mathbf{F}_{r_1}$ and $\mathbf{F}_{octa}$ depending on the threshold γ_0 chosen so as to maximize the minimum Euclidean distance. In [6], considering the outer FEC code and the turbo detection at the receiver, we studied the optimization of the switching threshold so as to lower the error-floor, *i.e.* to maximize I_{floor} (see Fig. 6). We showed that the MSEW mapping involved no switch in that case as beyond a given value of γ the criterion maximizing I_{floor} leads to the selection of $\mathbf{F}_{r1}$ only.

In this paper, we consider the maximization of $\ell_{\min}$ as the criterion to define the threshold γ_0 assuming the MSEW mapping. In Fig. 4, we plotted the value ℓ_{min} as a function of γ. We observe that $\gamma_1 = 30.7^o$ is the best threshold. Beneath γ_1 $\mathbf{F}_{r_1}$ outperforms $\mathbf{F}_{octa}$ and beyond γ_1, the trend is reversed. We define a new precoder from the newfound switching threshold γ_1: $\mathbf{F}_d = \mathbf{F}_{r_1}$ when $\gamma \leq \gamma_1$ and $\mathbf{F}_d = \mathbf{F}_{octa}$ otherwise. We refer to this new precoder as max-$\ell_{\min}$ precoder.

In Fig. 5, the probability density functions in terms of γ of different MIMO configurations are plotted for the case $b = 2$ data streams, where $n_d = |n_T - n_R|$. It is shown that the max-$\ell_{\min}$ precoder uses on average more $\mathbf{F}_{r1}$ form compared to the max-$d_{\min}$ precoder. In addition, we observe from Fig. 5 that the percentages of $17.28^o \leq \gamma \leq 30.7^o$ are 44.88%, 59.16% and 57.78% for $n_d = 0$, $n_d = 1$ and $n_d = 2$ respectively. In this interval ($17.28^o \leq \gamma \leq 30.7^o$), max-$d_{\min}$ uses $\mathbf{F}_{octa}$ while the max-$\ell_{\min}$ precoder uses $\mathbf{F}_{r1}$.

We conclude this section by mentioning that we plotted ℓ_{min} as a function of γ in the Gray-direct mapping case for both $\mathbf{F}_{r1}$ and $\mathbf{F}_{octa}$. We observed that both curves intersect at a value of γ roughly equal to γ_0. This study confirms the choice of γ_0 as the switching threshold for the Gray-direct mapping. The figure is not given in the paper due to space limitation.

C. Validation through EXIT chart

In this subsection, we use EXIT chart [9] to analyze the evolution of the MI between the bit-interleaved coded binary sequence $\bar{c}$ and its LLRs at input and output of the demapper when max-$d_{\min}$ and max-$\ell_{\min}$ are used. The extrinsic MI at output of demapper is a function of the *a priori* knowledge $\mathrm{I}_{\mathrm{A}}^1$ and the SNR. We define $\mathrm{I}_{\mathrm{E}}^1 = T_1\left(\mathrm{I}_{\mathrm{A}}^1, \mathrm{SNR}\right)$. Similarly, $\mathrm{I}_{\mathrm{E}}^2 = T_2(\mathrm{I}_{\mathrm{A}}^2)$. For details about the mathematical expressions of T_1 and T_2, the reader can refer to [9], [10]. The mutual information is averaged over 100 trials. Recall that the signal-to-noise ratio is defined by $\mathrm{SNR} = \frac{\sigma_s^2}{\sigma_\eta^2}\|\mathbf{H}\|_F^2 = \frac{\sigma_s^2}{\sigma_\eta^2}\rho^2$.

To demonstrate the difference between max-$\ell_{\min}$ and max-$d_{\min}$ precoders, let us randomly pick up a channel in the interval $17.28^o \leq \gamma \leq 30.7^o$ to plot the EXIT chart. Without loss of generality, we select $\gamma = 22^o$. We remind that, with this channel, max-$d_{\min}$ uses $\mathbf{F}_{octa}$ form while max-$\ell_{\min}$ uses $\mathbf{F}_{r1}$ form. Fig. 6 shows the EXIT chart of the iterative receiver over the selected channel ($\gamma = 22^o$) at SNR = 8 dB. The dashed line represents the EXIT function of the BCJR decoder of the $(13, 15)_{octa}$ RSC code, which is independent from SNR. Firstly, it is observed that using Gray-like mapping results in an early crossing between the two EXIT functions and leads to worse error-rate performance. This, again, confirms the advantage of MSEW compared to the conventional Gray-like mapping. Secondly, by considering MSEW mapping, we observe that the tunnel of the EXIT chart is wider in the case of max-$\ell_{\min}$ precoder ($\mathbf{F}_{r1}$ + MSEW) than in the case of max-$d_{\min}$ ($\mathbf{F}_{octa}$ + MSEW). This predicts a better error-rate performance at the turbo-cliff region. The ending point (I_{floor}) of the EXIT function of max-$\ell_{\min}$ is also higher than the one of max-$d_{\min}$, which predicts a better performance at the error-floor by using max-$\ell_{\min}$.

IV. Simulation results

Monte-Carlo simulation has been carried out over random MIMO channels, *i.e.* each element of $\mathbf{H}$ is distributed as $\mathrm{H}_{i,j} \sim \mathcal{CN}(0, 1)$. Thus, on average, each channel element has unit energy, *i.e.* $\mathrm{E}[|\mathrm{H}_{ij}|^2] = 1$. Note that, with the definition of instantaneous SNR in (4), the error-rate performance does not depend on ρ^2. Therefore, the system performance for different values of γ is obtained by taking the average of the randomly generated channels. The half-rate $(13, 15)_{octal}$-RSC code is used as FEC encoder. The frame length is set to 800 uncoded bits and interleaved by a random interleaver.

Fig. 7 shows the average bit-error-rate (BER, in solid lines) and frame-error-rate (FER, in dashed lines) performances of the considered system over random 2×2 MIMO channels. Firstly, the error-rate performance in case max-$d_{\min}$ precoder is used with Gray-like mapping is plotted to compare with the case max-$d_{\min}$ used with MSEW mapping. As observed, in terms of FER, the MSEW-mapped max-$d_{\min}$ achieves a gain of roughly 1.5 dB at FER = 10^{-2} compared to the Gray-like mapped max-$d_{\min}$. The gain is even more significant at high SNR due to slope changes of the FER curves. In terms of BER, at high SNR, the gain is roughly 0.8 dB at BER= 10^{-4}. At low SNR, BER performance of Gray-direct is better than that of MSEW, which is in accordance with the EXIT chart analysis, since the corresponding EXIT function of Gray-direct mapping begins higher and, therefore, it avoids intersection at the bottleneck. This also makes the gap between the FER and BER of Gray-direct mapping is larger than that of MSEW

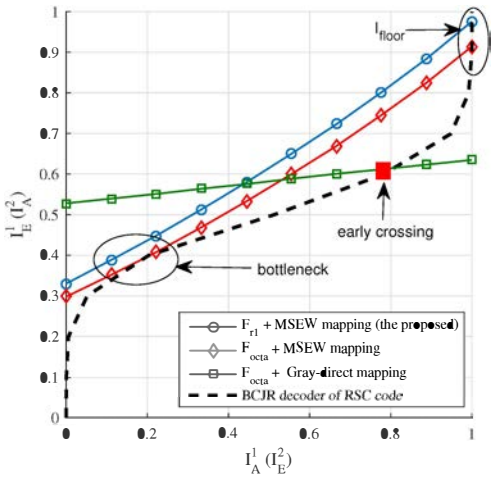

Fig. 6: EXIT chart for the iterative receiver used with different precoders and the associated mappings, $\gamma = 22^o$, SNR = 8 dB, RSC(13,15).

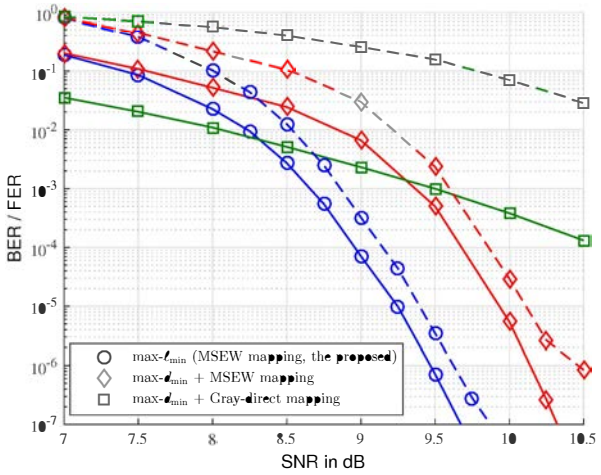

Fig. 7: Average BER (solid lines) and FER (dashed lines) performance of the precoded turbo detection over random 2×2 MIMO channels.

mapping as observed in Fig. 7. However, in terms of FER performance, MSEW still achieves a gain, even at low SNR. This is due to the early crossing of the EXIT function of the Gray-direct mapping and the EXIT function of decoder (see Fig. 6). The results above show the advantage of MSEW mappings for max-$d_{\min}$ precoder over random channels.

Secondly, we observe from Fig. 7 that the performance gains are even more significant when max-$\ell_{\min}$ is used. Precisely, in terms of BER, max-$\ell_{\min}$ precoder achieves the gains of more than 1.5 dB and roughly 0.75 dB compared to Gray-like mapped and MSEW-mapped max-$d_{\min}$ respectively. As demonstrated in Fig. 6, with MSEW mapping, the corresponding EXIT function of max-$\ell_{\min}$ precoder is higher than the one of max-$d_{\min}$ precoder at both bottleneck and I_{floor} regions. This results in the performance gains of max-$\ell_{\min}$ compared to MSEW-mapped max-$d_{\min}$ at any value of the considered SNR range, as demonstrated in Fig. 7.

It is essential to emphasize that since the max-$\ell_{\min}$ aims to maximize $\ell_{\min}$, the performance gain of max-$\ell_{\min}$ compared max-$d_{\min}$ is even more significant at high SNR, where the errors mostly occur due to wrong detection between pairs of symbols, whose binary patterns differ by exactly one bit. Indeed, as shown in Fig. 7, at FER = 10^{-6}, while the FER curve of max-$\ell_{\min}$ continues to go down, the FER curve of MSEW-mapped max-$d_{\min}$ begins to saturate.

V. Conclusion

In this paper we focused on the design of precoders assuming an outer FEC code and a turbo detection at the receiver. We considered the two forms of the max-$d_{\min}$ precoder [5] with the MSEW mapping defined in [6]. We optimized the switching threshold so as to maximize the minimum Euclidean distance between two received sequences whose associated binary sequences differ by one position. We referred to the optimized precoder as max-$\ell_{\min}$. Simulations (EXIT chart and BER performance) showed the improvement achieved by max-$\ell_{\min}$ compared to max-$d_{\min}$. Future works will consider the optimization of the generic expression of $\mathbf{F}_d$ according to the maximization of ℓ_{min}.

Acknowledgment

The authors would like to acknowledge Dr. Robert G. Maunder, University of Southampton, UK, for the helpful discussion about EXIT chart analysis.

References

[1] Q. Li, G. Li, W. Lee, M. Lee, D. Mazzarese, B. Clerckx, and Z. Li, "MIMO techniques in WiMAX and LTE: a feature overview," *IEEE Commun. Mag.*, vol. 48, no. 5, pp. 86–92, 2010.

[2] C. Berrou and A. Glavieux, "Near optimum error correcting coding and decoding: Turbo-codes," *IEEE Trans. on Commun.*, vol. 44, no. 10, pp. 1261–1271, 1996.

[3] A. Picart, P. Didier, and A. Glavieux, "Turbo-detection: a new approach to combat channel frequency selectivity," in *IEEE Int. Conf. on Commun. Towards the Knowledge Millennium*, vol. 3, 1997, pp. 1498–1502.

[4] S. Haykin, M. Sellathurai, Y. de Jong, and T. Willink, "Turbo-MIMO for wireless communications," *IEEE Commun. Mag.*, vol. 42, no. 10, pp. 48–53, 2004.

[5] L. Collin, O. Berder, P. Rostaing, and G. Burel, "Optimal minimum distance-based precoder for MIMO spatial multiplexing systems," *IEEE Trans. on Signal Processing*, vol. 52, no. 3, pp. 617–627, 2004.

[6] N.-Q. Nhan, P. Rostaing, K. Amis, L. Collin, and E. Radoi, "Optimized MIMO symbol mapping to improve the turbo cliff region of iterative precoded MIMO detection," in *EUSIPCO*, 2015, pp. 909–913.

[7] L. Bahl, J. Cocke, F. Jelinek, and J. Raviv, "Optimal decoding of linear codes for minimizing symbol error rate," *IEEE Trans. on Info. Theory*, pp. 284–287, Mar. 1974.

[8] J. Tan and G. L. Stuber, "Analysis and design of symbol mappers for iteratively decoded bicm," *IEEE Trans. on Wireless Commun.*, vol. 4, no. 2, pp. 662–672, 2005.

[9] J. Hagenauer, "The exit chart-introduction to extrinsic information transfer in iterative processing," in *EUSIPCO*, 2004, pp. 1541–1548.

[10] S. Ten-Brink, "Designing iterative decoding schemes with the extrinsic information transfer chart," *AEU Int. J. Electron. Commun.*, vol. 54, no. 6, pp. 389–398, 2000.